AIP Journal of Applied Physics

Comparative study of polar and semipolar ($11\bar{2}2$) InGaN layers grown by metalorganic vapour phase epitaxy

Duc V. Dinh, F. Oehler, V. Z. Zubialevich, M. J. Kappers, S. N. Alam, M. Caliebe, F. Scholtz, C. J. Humphreys, and P. J. Parbrook

Citation: Journal of Applied Physics **116**, 153505 (2014); doi: 10.1063/1.4898569
View online: http://dx.doi.org/10.1063/1.4898569
View Table of Contents: http://scitation.aip.org/content/aip/journal/jap/116/15?ver=pdfcov
Published by the AIP Publishing

[This article is copyrighted as indicated in the article. Reuse of AIP content is subject to the terms at: http://scitation.aip.org/termsconditions. Downloaded to] IP: 143.239.65.254 On: Thu, 16 Oct 2014 14:24:00

JOURNAL OF APPLIED PHYSICS **116**, 153505 (2014)

Comparative study of polar and semipolar $(11\bar{2}2)$ InGaN layers grown by metalorganic vapour phase epitaxy

Duc V. Dinh,[1,a)] F. Oehler,[2] V. Z. Zubialevich,[1] M. J. Kappers,[2] S. N. Alam,[1,3] M. Caliebe,[4] F. Scholtz,[4] C. J. Humphreys,[2] and P. J. Parbrook[1,3,a)]
[1]*Tyndall National Institute, University College Cork, Lee Matltings, Dyke Parade, Cork, Ireland*
[2]*Department of Materials Science and Metallurgy University of Cambridge, Pembroke Street, Cambridge CB2 3QZ, United Kingdom*
[3]*School of Engineering, University College Cork, Cork, Ireland*
[4]*Institute of Optoelectronics, Ulm University, Ulm 89069, Germany*

(Received 2 July 2014; accepted 7 October 2014; published online 16 October 2014)

InGaN layers were grown simultaneously on $(11\bar{2}2)$ GaN and (0001) GaN templates by metalorganic vapour phase epitaxy. At higher growth temperature ($\geq$750 °C), the indium content (<15%) of the $(11\bar{2}2)$ and (0001) InGaN layers was similar. However, for temperatures less than 750 °C, the indium content of the $(11\bar{2}2)$ InGaN layers (15%–26%) were generally lower than those with (0001) orientation (15%–32%). The compositional deviation was attributed to the different strain relaxations between the $(11\bar{2}2)$ and (0001) InGaN layers. Room temperature photoluminescence measurements of the $(11\bar{2}2)$ InGaN layers showed an emission wavelength that shifts gradually from 380 nm to 580 nm with decreasing growth temperature (or increasing indium composition). The peak emission wavelength of the $(11\bar{2}2)$ InGaN layers with an indium content of more than 10% blue-shifted a constant value of $\approx$(50–60) nm when using higher excitation power densities. This blue-shift was attributed to band filling effects in the layers. © *2014 AIP Publishing LLC*. [http://dx.doi.org/10.1063/1.4898569]

I. INTRODUCTION

The fabrication of light-emitting devices (LEDs) based on semipolar oriented III-nitride semiconductor compounds (AlN, GaN, and InN) has gained much interest due to the predicted reduction of polarization effects (PEs) due to the tilting of the energy band edges.[1] The reduction of PEs increases overlap between electron and hole wave-functions resulting in an increase of radiative recombination probability, which may overcome the "green gap" problem as well as enhance the performance of LEDs based on semi-polar nitrides.[2,3] Efficient green and yellow semipolar $(11\bar{2}2)$ InGaN single quantum-well LEDs grown on free-standing $(11\bar{2}2)$ GaN substrates with threading dislocation densities below $10^7\,\mathrm{cm}^{-2}$ have been recently demonstrated.[4,5] However, the free-standing GaN substrates required for this approach remain small and expensive. Therefore, hetero-epitaxially grown semipolar structures continue to be of interest due to the much lower cost and larger substrate sizes available. However, a major disadvantage of the latter approach is the potentially detrimental contribution of high defect densities of threading dislocations (typically $\approx 10^{10}\,\mathrm{cm}^{-2}$) and basal plane stacking faults (BSFs) ($\approx 10^5\,\mathrm{cm}^{-1}$).[6,7] It has been shown that the high density of BSFs affects the optical and electrical properties of the layers, e.g., increasing the non-radiative recombination rate[8] and causing an electrical anisotropy via the carrier scattering from BSFs.[9]

It is particularly interesting regarding the application for green and yellow light emitters that an increased indium incorporation on the $(11\bar{2}2)$ surface was predicted from first-principles calculations by Northrup,[10] who argued that the strain-repulsive interaction between In-atoms in GaN is weaker on the $(11\bar{2}2)$ surface than on the nonpolar $(10\bar{1}0)$ *m*-plane surface. A higher indium incorporation for semipolar planes than for the basal plane was predicted from two-dimensional modelling of metalorganic vapour phase epitaxy (MOVPE) in a vertical reactor,[11,12] with a distinct maximum indium incorporation for $(11\bar{2}2)$ InGaN, attributed to a minimum in strain energy. The few reported comparative MOVPE growth studies suggest that semipolar $(11\bar{2}2)$ have a higher indium incorporation rate than polar and nonpolar planes,[2,13,14] or demonstrate that indium incorporation is virtually independent of the growth plane.[15] In contrast, $(11\bar{2}2)$ InGaN epilayers grown by plasma-assisted molecular beam epitaxy (PAMBE)[16] and ammonia-MBE (Ref. 17) show the opposite trend, whereby the (0001) films had a higher indium incorporation. Das *et al.*[16] proposed that the decreased indium incorporation was related to the surface roughness of the semi-polar surface, but the smooth surface maintained in the study by Browne *et al.* indicates that the low indium incorporation is more likely related to the conditions used for MBE growth.[17]

Here, we have conducted a study on the MOVPE growth of 25–30 nm-thick InGaN layers simultaneously on $(11\bar{2}2)$ and (0001) GaN templates as a function of the InGaN growth temperature. As already pointed out by Jönen *et al.*,[15] it is imperative to use detailed x-ray diffraction (XRD) analysis methods to determine the alloy composition and the strain state of the films, which has recently become more accessible for semi-polar structures.[18] In this context, we have elected to study first InGaN epilayers rather than thin quantum well systems in order to simplify the structural and optical analysis. Thus, we report here on the comparative characterization of simultaneously grown $(11\bar{2}2)$ and (0001) InGaN epilayers

a)Electronic addresses: vanduc.dinh@tyndall.ie and peter.parbrook@tyndall.ie

 © 2014 AIP Publishing LLC

[This article is copyrighted as indicated in the article. Reuse of AIP content is subject to the terms at: http://scitation.aip.org/termsconditions. Downloaded to] IP: 143.239.65.254 On: Thu, 16 Oct 2014 14:24:00

as a function of InGaN growth temperature to vary the alloy composition. We found that at growth temperatures higher than 750 °C, the indium contents of the $(11\bar{2}2)$ and (0001) InGaN layers were similar, while at growth temperatures lower than 750 °C, the indium content of the $(11\bar{2}2)$ InGaN layers was lower than that of the (0001) InGaN layers, an effect attributed to the relaxation state of the layers.

II. EXPERIMENTAL DETAILS

Growth was performed in an Aixtron 3×2 in. close-coupled showerhead MOVPE reactor. Trimethylgallium (TMGa), trimethylindium (TMIn), and ammonia (NH_3) precursors were used as Ga, In, and N sources, respectively. InGaN layers were grown in the temperature range of 675–825 °C on 2-in. wafer quarters of MOVPE-grown $(11\bar{2}2)$ GaN buffer layers deposited on *m*-plane sapphire substrates. The MOVPE growth of the $(11\bar{2}2)$ GaN templates is reported elsewhere,[19] with samples exhibiting typical threading dislocation and BSF densities of $(3.0 \pm 0.2) \times 10^{10}\,\mathrm{cm}^{-2}$ and $(3.2 \pm 0.3) \times 10^{5}\,\mathrm{cm}^{-1}$, respectively.[7] InGaN layers were also simultaneously grown on (0001) GaN templates for comparison. The (0001) GaN templates were grown on high temperature AlN templates that were deposited on *c*-plane sapphire.[20] The threading dislocation density of the *c*-plane GaN templates was typically $\approx(2.5\text{–}4.0) \times 10^{8}\,\mathrm{cm}^{-2}$ as determined by XRD and atomic force microscope (AFM) measurements.

A GaN connecting layer with a thickness of 450 nm was grown at 1040 °C on the GaN templates prior to InGaN deposition. For the growth of the GaN, hydrogen was used as the carrier gas, and the reactor pressure was 100 hPa. The reactor ambient was then switched to nitrogen at a pressure of 400 hPa during cooling to 675–825 °C, corresponding to the InGaN growth temperature measured by a Laytec *in-situ* pyrometer. The InGaN layers were grown on the GaN templates using a TMIn flux of 5.7 μmol/min and a TMGa flux of 8.2 μmol/min. The NH_3 flux was maintained at 134 mmol/min in all cases. The uncapped InGaN layer thickness was kept between 25 nm and 30 nm.

The crystalline properties of the InGaN samples were characterized using a PANalytical X'pert triple-axis high-resolution XRD (HRXRD) system with a $\mathrm{CuK}_{\alpha 1}$ source. The surface morphology of the InGaN layers was investigated using a Veeco MultiMode V AFM in tapping mode. Photoluminescence (PL) measurements of the InGaN layers were measured using a Horiba iHR320 spectrometer using two different continuous-wave (CW) lasers: He-Cd (325 nm) and Ar^{+}-ion (244 nm) with power densities of 0.5 W/cm^2 and 5.0 W/cm^2, respectively. A monochromator coupled Xe-lamp (450 W) was used as the excitation source for PL excitation (PLE) measurements. Additional PL measurements were performed using an Accent RPM2000 mapping system equipped with a 266 nm Q-switched laser giving a peak excitation power density of 1.0 MW/cm^2.

The indium content of the (0001) InGaN samples was calculated using the PANalytical X'Pert Epitaxy software based on the *c*- and *a*-cell parameters determined by the (0002) and $(10\bar{1}5)$ reflections, respectively. The indium content of the $(11\bar{2}2)$ InGaN layers was determined using the recently developed XRD analysis method of Oehler *et al.*[18] The experimental error in indium content is estimated to be around 1.0% for layers of this thickness.[18,21]

III. RESULTS AND DISCUSSION

A. Surface morphology

The AFM determined surface morphology of all the $(11\bar{2}2)$ InGaN layers shows undulation along $[1\bar{1}00]$, very

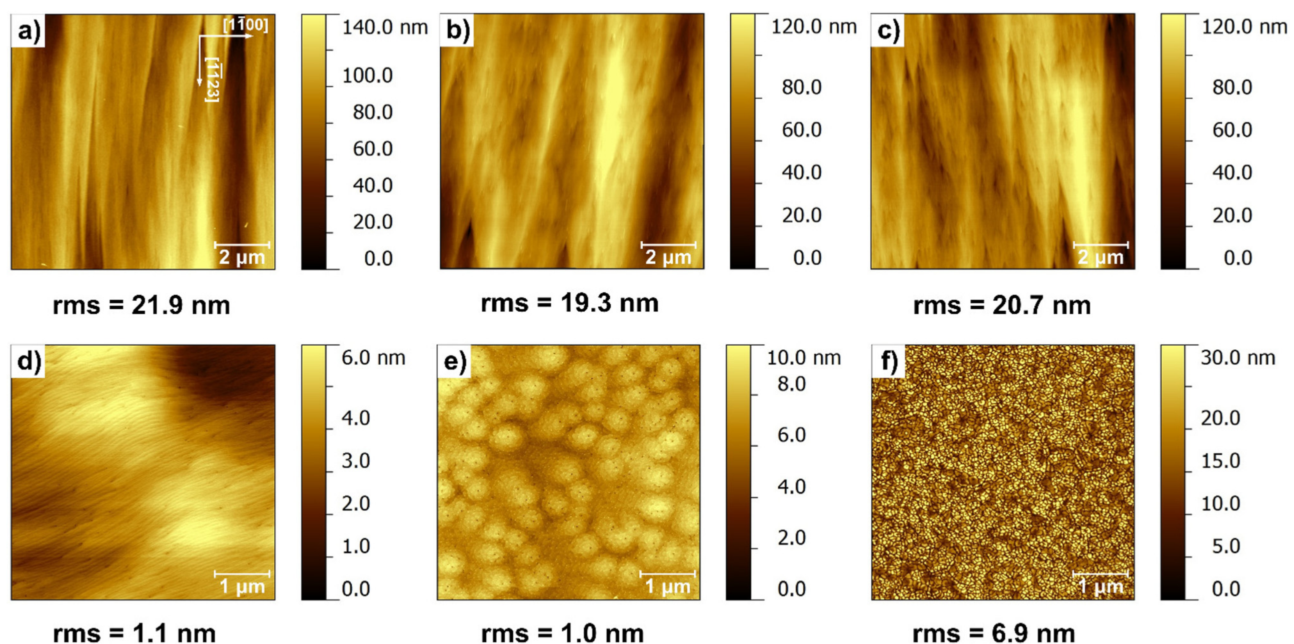

FIG. 1. (Top row) AFM images ($10 \times 10\,\mu\mathrm{m}^2$) of a $(11\bar{2}2)$ GaN layer template (a) and $(11\bar{2}2)$ InGaN layers grown at (b) 775 °C and (c) 675 °C. (Bottom row) AFM images ($5 \times 5\,\mu\mathrm{m}^2$) of a (0001) GaN layer template (d) and (0001) InGaN layers grown at (e) 775 °C and (f) 675 °C. The root-mean square (rms) roughness values of each images are shown for comparison.

[This article is copyrighted as indicated in the article. Reuse of AIP content is subject to the terms at: http://scitation.aip.org/termsconditions. Downloaded to] IP: 143.239.65.254 On: Thu, 16 Oct 2014 14:24:00

similar to the underlying GaN templates, as can be observed in Fig. 1. The root-mean square (rms) roughness values of the $(11\bar{2}2)$ InGaN and GaN were both about 20 nm for a scan size of $10 \times 10\,\mu m^2$. The formation of the corrugated surface morphology on $(11\bar{2}2)$ InGaN/GaN grown on *m*-plane sapphire is attributed to the anisotropic diffusion of group-III atoms on the $(11\bar{2}2)$ and *m*-plane surfaces.[22,23] In contrast to the unchanging morphology of the $(11\bar{2}2)$ InGaN layers, the surface morphology of the simultaneously grown (0001) InGaN layers changed from the step flow surface observed for GaN (Fig. 1(d)) to spiral-like InGaN growth above 725 °C, as shown in Fig. 1(e), and then to island-like for InGaN temperatures lower than this value, as can be observed in Fig. 1(f).

The (0001) InGaN layers exhibit high densities of dark-/V-pits, which are likely to be screw dislocations, on the surface $\approx 8 \times 10^8\,cm^{-2}$ as estimated for the sample grown at 775 °C (see Fig. 1(e), for instance); although the areas between these pits are much smoother. Since the V-pits ($\approx 3 \times 10^8\,cm^{-2}$) were also observed on the (0001) GaN templates (Fig. 1(d)), the V-pits on the (0001) InGaN surfaces might be derived from the templates. V-pit formation is thus likely to be due to the existence of threading defects, i.e., the V-pits are initiated when dislocation cores open up during the low temperature InGaN growth.[24] The low InGaN growth temperature (675–850 °C) causes poor surface migration of In- and Ga-atoms to completely form a layer-by-layer growth and hence form additional V-pits; thus, the V-pits are stabilized in this temperature regime. For the $(11\bar{2}2)$ InGaN layers, no surface pits are formed despite the defect density being higher. The most likely reason is that in this temperature regime the $(11\bar{2}2)$ surface is also stabilized like the $(10\bar{1}1)$ surface.[24]

In this section, the surface morphology of the InGaN layers was studied. The morphology of the $(11\bar{2}2)$ InGaN/GaN layers was found to be similar to the underlying GaN templates (Fig. 1). This undulated morphology is attributed to the anisotropic diffusion of group-III atoms on the $(11\bar{2}2)$ surface.[22,23] In contrast, the surface morphology of the (0001) InGaN/GaN layers changed from step flow (775–825 °C) to spiral-like (725–750 °C) and finally to an island-like surface (675–700 °C). This was attributed to the lower surface migration[24] of In- and Ga-atoms with decreasing growth temperature and to the strain relaxation of the samples (see Table I).

B. Composition and crystalline properties

To determine the indium content of the $(11\bar{2}2)$ InGaN layers and the strain state of the layers, we measured XRD reciprocal space maps (RSM) of symmetric and asymmetric reflections along the two in-plane directions $[1\bar{1}00]$ and $[\bar{1}\bar{1}23]$: $(11\bar{2}2)_{[\bar{1}100]}$, $(11\bar{2}2)_{[11\bar{2}3]}$, $(11\bar{2}4)_{[\bar{1}100]}$, and $(21\bar{3}3)_{[11\bar{2}3]}$. For (0001) oriented layers, a single asymmetric reflection $(10\bar{1}5)$ was used to assess the strain state of the layer.

From the RSMs of the $(11\bar{2}2)$ InGaN layers, the tilt angle along $[\bar{1}\bar{1}23]$ with respect to the $(11\bar{2}2)$ GaN templates was determined. The tilt angle of the $(11\bar{2}2)$ InGaN layers increased with decreasing growth temperature (increasing indium content), and seems to correlate with the strain relaxation (Table I).

The indium content and the degree of relaxation of the $(11\bar{2}2)$ InGaN layers were determined from symmetric RSM of the $(11\bar{2}2)$ reflection along $[\bar{1}\bar{1}23]$. The measurement method has been described in detail in Ref. 18 and takes into account the tilt of the InGaN layer (Table I). The measurement also assumes that the layers are fully strained along $[1\bar{1}00]$ and that partial relaxation can only occur along the $[\bar{1}\bar{1}23]$ direction through dislocation glide on the basal plane (i.e., 1D relaxation).[18] From the XRD data, it is observed that the $(11\bar{2}2)$ InGaN layer loses coherency at growth temperatures less than 800 °C, but is still only partially relaxed at the lowest growth temperature of 675 °C. Zhao *et al.*[13] observed that partial relaxation set in at an In-content of about 6% for 20 nm-thick $(11\bar{2}2)$ InGaN films grown on free-standing GaN substrates, which is in good agreement with our findings. In contrast, the (0001) InGaN layer remains coherent down to a growth temperature of 750 °C. Below that growth temperature, the (0001) InGaN layer rapidly changes to an essentially fully relaxed state over a relatively narrow temperature range of 50 °C.

Figure 2 shows graphically the alloy composition and the strain relaxation status (as determined from XRD) of the $(11\bar{2}2)$ and (0001) InGaN layers as a function of growth temperature (see also Table I). In general, the indium content of the layers increases with decreasing growth temperature due to the reduction of indium desorption rate. At the higher growth temperatures (≥750 °C), the indium contents (<15%) of the $(11\bar{2}2)$ and (0001) InGaN layers are similar, while at the lower growth temperatures (<750 °C), the

TABLE I. Strain relaxation and In-content (±1.0%) of the (0001) InGaN and $(11\bar{2}2)$ InGaN layers grown at different temperatures.

		InGaN growth temperature (°C)						
Orientation	Calculated parameter	825	800	775	750	725	700	675
(0001)	Relaxation (%)	0	0	0	0	80	100	100
	In-content (%)	3.0	5.7	9.4	14.8	26.1	32.0	31.0
$(11\bar{2}2)$	Relaxation (%)	0	0	10	30	44	63	73
	In-content (%)	2.0	…	10.4	15.2	18.0	21.7	23.0
	Tilt angle (°) (along $[\bar{1}\bar{1}23]$)	0	…	0.2	0.5	0.8	1.4	1.7

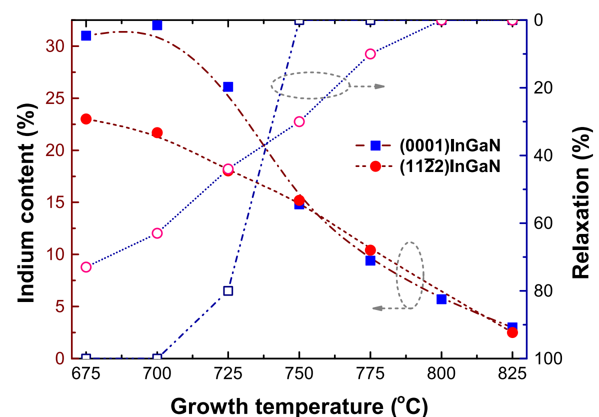

FIG. 2. The XRD-calculated indium content and relative strain relaxation status of the (0001) InGaN (■) and $(11\bar{2}2)$ InGaN layers (·) grown at different temperatures (see text for details).

[This article is copyrighted as indicated in the article. Reuse of AIP content is subject to the terms at: http://scitation.aip.org/termsconditions. Downloaded to] IP: 143.239.65.254 On: Thu, 16 Oct 2014 14:24:00

indium content of the $(11\bar{2}2)$ InGaN is consistently lower than that of the (0001) layers.

Thus, the (0001) InGaN composition starts to deviate from that of the semi-polar layers at the onset of rapid (0001) strain relaxation below a growth temperature of 750 °C (Fig. 2). At that growth temperature of 750–725 °C, the corresponding $(11\bar{2}2)$ InGaN film is already partially relaxed (between 30% and 44%). The effect of this partial relaxation on the indium incorporation is unknown but since the trend of increasing indium content with reducing temperature continues unchanged below 750 °C, this effect is likely to be small. Additionally, it is worth noting that the surface morphology of the (0001) InGaN layers also altered with the change of growth temperature (Fig. 1), while the surface morphology of the $(11\bar{2}2)$ InGaN layers remained unchanged. Theoretically, it was found that indium distribution in InGaN/GaN islands strongly depends on subsurface diffusion, whereby indium atoms tend to occupy the outmost island surface layer.[25] Thus, the island-like surface morphology together with the strain relaxation of the grown (0001) InGaN layers (<750 °C) were attributed to the enhanced In incorporation, while the constant surface morphology of the $(11\bar{2}2)$ InGaN layers did not induce a significant change in compositional trend.

The lower composition of the $(11\bar{2}2)$ InGaN layers compared to the (0001) InGaN layers at growth temperatures below 750 °C is in disagreement with theoretical calculations that predict higher incorporation rates on the $(11\bar{2}2)$ surface.[10–12] This results here also contradict previous reports on MOVPE-grown $(11\bar{2}2)$ InGaN.[2,13–15] The different compositions may be due to different growth parameters[13–15] or different calculation methods, e.g., with[14,18] and without[13] taking the strain state into account.

The anisotropic crystallinity (the full-width at half maximum (FWHM) values of the on-axis XRD rocking curves (XRC)) of semi-/non-polar nitrides is commonly observed,[7,22,23,26,27] and it is mainly due to the anisotropic growth and the unequal distribution of dislocations.[22,23] For semipolar $(11\bar{2}2)$ nitrides (e.g., InN,[23,26] GaN,[7] and AlGaN[27]), the XRC FWHM value was found to be larger along $[1\bar{1}00]$ than along $[\bar{1}\bar{1}23]$.

Figure 3 shows the on-axis XRC FWHM values measured along both in-plane directions of the $(11\bar{2}2)$ InGaN layers. The (0002) XRC FWHM values of the (0001) InGaN layers are plotted for comparison. For reference, the XRC FWHM values of the $(11\bar{2}2)$ GaN templates were 0.28° along $[1\bar{1}00]$ and 0.2° along $[\bar{1}\bar{1}23]$. The XRC FWHM values of the InGaN layers increased with decreasing growth temperature, indicating a reduced crystal quality. Interestingly, the XRC FWHM values along $[\bar{1}\bar{1}23]$ were found to be larger than the values along $[1\bar{1}00]$ at the temperature range of 700–775 °C. This change was attributed to the change of strain relaxation status of the layers (Table I, and Figs. 2 and 3). In the applied XRD measurement method for the determination of indium content, the layers were assumed to be fully strained along $[1\bar{1}00]$;[18] it is expected that some partial relaxation occurred along that direction when the layers were grown below 725 °C due to a small shift along $[1\bar{1}00]$ of the $(\bar{2}\bar{1}33)$ InGaN reflection with respect to the $(\bar{2}\bar{1}33)$ GaN

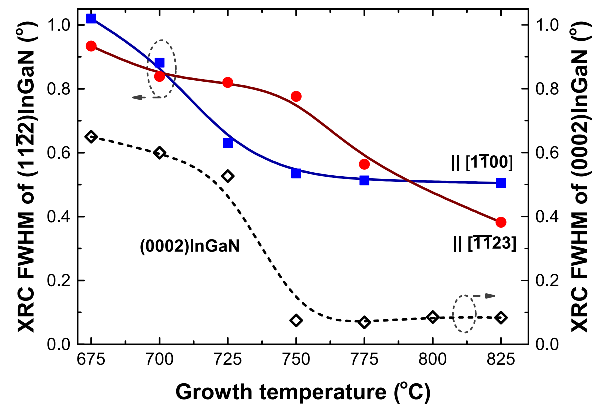

FIG. 3. The on-axis XRC FWHM values of the (0001) InGaN layers (◇), and the $(11\bar{2}2)$ InGaN layers scanned along $[1\bar{1}00]$ (■) and $[\bar{1}\bar{1}23]$ (●) grown at different temperatures.

reflection. Consequently, the layer may start to relax along $[1\bar{1}00]$ (≈725 °C), the XRC FWHM values increase and then reach a larger value than along $[\bar{1}\bar{1}23]$ (<700 °C). The expected partial relaxation along $[1\bar{1}00]$ of the $(11\bar{2}2)$ InGaN layers grown at below 725 °C may lead to a change of average composition. To clarify this expectation, further investigation will be needed.

In the case of the (0001) InGaN layers, the XRC FWHM value (≈0.1°) of the fully strained (0001) InGaN layer (≥750 °C) is comparable to that for the (0001) GaN template, while the relaxed layer has much larger XRC FWHM value, e.g., ≈0.53° for the sample grown at below 725 °C (Fig. 3). This indicates that new threading dislocations were generated in the relaxed (0001) InGaN layers (≤725 °C), and hence broadened the XRC scans.

In this section, the composition and crystal quality of the $(11\bar{2}2)$ and (0001) InGaN/GaN layers are discussed. For InGaN growth temperature >750 °C, the indium incorporation on the two orientations was similar, whereas at lower temperatures, a divergence was observed, with the (0001) layers having higher indium content. This is attributed to the rapid change in morphology and strain state for these samples. As expected, the crystal quality in both cases decreased with decreasing growth temperature.

C. Optical properties

The room-temperature luminescent properties of the InGaN layers were investigated using three different excitation sources. For the (0001) InGaN layers, no near band-edge (NBE) luminescence related to InGaN was observed when using the weakest 325 nm CW excitation source. Instead, only a broad band at ≈560 nm was found,[28] which most probably corresponds to the yellow luminescence of (0001) InGaN and GaN. Using the 244 nm CW excitation source, weak NBE luminescence related to the (0001) InGaN layers could be observed for In ≥10%. Under the high intensity pulsed excitation at 266 nm, clear NBE luminescence was observed for the samples with In-content up to 15%, which matches the point of relaxation in the (0001) InGaN samples. The RT-PL peak emission wavelength of the fully strained (0001) InGaN layers (3% ≥ In ≥ 15%)

[This article is copyrighted as indicated in the article. Reuse of AIP content is subject to the terms at: http://scitation.aip.org/termsconditions. Downloaded to] IP: 143.239.65.254 On: Thu, 16 Oct 2014 14:24:00

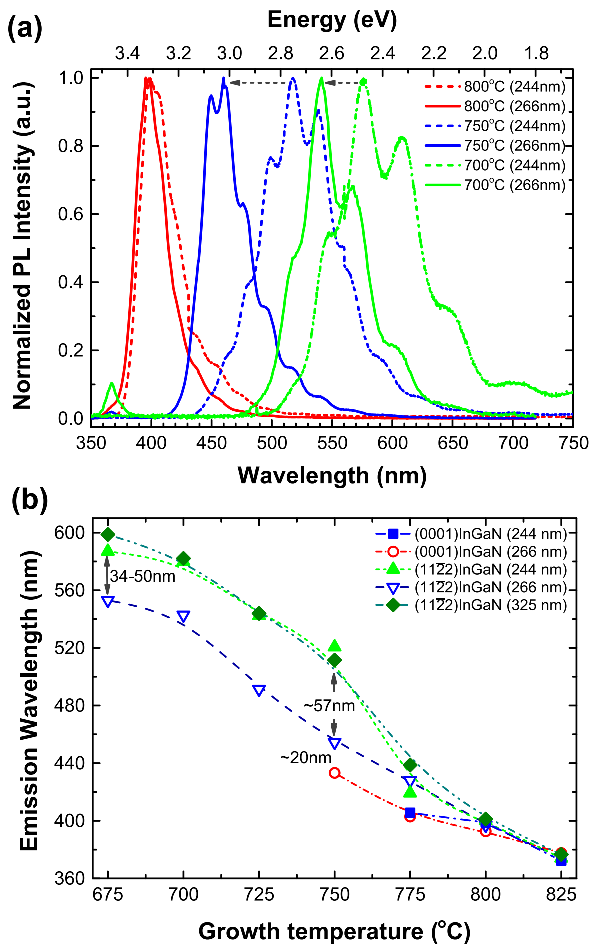

FIG. 4. (a) RT-PL spectra measured with 244 nm CW (dashed lines) and 266 nm (solid lines) pulsed excitation lasers of the (11$\bar{2}$2) InGaN layers grown at different temperatures. (b) The RT-PL peak emission wavelength of the (0001) and (11$\bar{2}$2) InGaN layers measured with 325, 244, and 266 nm excitation sources.

varied from 377 nm to 433 nm (Fig. 4(b)). However, the (0001) InGaN layers grown below 750 °C (In > 15%) did not show NBE emission, but evidence of defect-related luminescence was observed.

The (11$\bar{2}$2) InGaN layers showed NBE luminescence at room temperature (Fig. 4) irrespective of the excitation source used. The much higher PL intensity of the (11$\bar{2}$2) InGaN layers than that for the (0001) InGaN layers might be due to background doping and/or carrier localization effects. It is well-known that impurities such as oxygen may be unintentionally incorporated into the III-nitride films during growth, making the films *n*-type in nature. For *n*-type GaN, e.g., *c*-plane Si:GaN,[29–31] the PL intensity of NBE GaN was found to be increased with increasing doping concentration. Recently, it has been reported that the oxygen incorporates into InGaN and GaN layers during growth ($>10^{18}$ cm^{-3}) is much higher in the (11$\bar{2}$2) and (11$\bar{2}$0) oriented material than that for the (0001) orientation ($<1\times10^{17}$ cm^{-3}).[17,32] Secondary ion mass spectrometry measurements were performed on our InGaN samples and found that O-concentration was about 1×10^{18} cm^{-3} for (11$\bar{2}$2) InGaN and less than 1×10^{17} cm^{-3} for (0001) InGaN. Thus, the high oxygen impurity incorporation may enhance the PL intensity of the (11$\bar{2}$2) InGaN samples compared to the (0001) InGaN samples.

In addition to the enhanced PL intensity of the (11$\bar{2}$2) InGaN layers caused by the O-incorporation, the enhanced PL intensity might be also due to the localization effects.[33] Carrier localization effects might be derived from self-organized indium-rich InGaN regions (i.e., deviations from randomness). Carrier localization can prevent carriers from reaching defects, leading to a reduction of non-radiative recombination rates. In the case of the (0001) InGaN layers, a very high density of pits was observed on the surface, associated with dislocations in InGaN that are non-radiative centers.[34] Using low excitation powers, most carriers will be trapped in the non-radiative centers, resulting in the defect related luminescence of the (0001) samples. High excitation powers can lead to a partial saturation of the trap luminescence with the excess carriers able to radiatively recombine at the (0001) InGaN NBE. However, when the (0001) InGaN layers are relaxed (>15%), the defect densities increase leading in turn to an increase in non-radiative recombination causing elimination of the NBE luminescence even at elevated excitation power.

Figure 4(a) shows the normalized RT-PL spectra of the (11$\bar{2}$2) InGaN layers grown at different temperatures measured with the 244 nm and 266 nm excitation sources. The RT-PL peak emission wavelengths are almost the same for the 325 nm and 244 nm CW lasers. However, a blue-shift up to 60 nm of luminescence was observed by using the 266 nm excitation source. Multiple interference peaks are clearly observed due to the presence of the Fabry-Pérot effect in the sapphire/epilayer/air cavity.[35] Furthermore, no yellow luminescence attributed to the GaN templates was observed for the (11$\bar{2}$2) InGaN samples, consistent with the data obtained on the as-grown (11$\bar{2}$2) GaN templates. However, a weak luminescence band at longer 650 nm was observed and that is attributed to defects in the (11$\bar{2}$2) GaN and InGaN layers.

The NBE PL peak emission wavelength (estimated from Gaussian fit of the corresponding band) of the (0001) and (11$\bar{2}$2) InGaN layers measured by the different excitation sources are shown in Fig. 4(b). For In <5.7% (800–825 °C), both layers have similar NBE PL peak emission wavelength (≈375–400 nm). Within the range of 5.7% ≥ In ≥ 15% (800–750 °C), even though the (0001) InGaN layers have similar indium content (Fig. 2), the peak emission wavelength of the (11$\bar{2}$2) InGaN layers shifts to longer wavelength than that for the (0001) InGaN layers. The red-shift of the (11$\bar{2}$2) InGaN NBE may be due to the presence of BSFs, typically at a high density in hetero-epitaxially grown semi-/non-polar films; however, only a 10 nm shift is observed for (11$\bar{2}$2) GaN.[6] The red-shift of the (11 22) InGaN NBE might be also due to the stronger carrier localization.[33] It is worth noting that recently we compared the RT-PL peak emission wavelength (244 nm and 325 nm excitation sources) of InGaN materials grown on different (11$\bar{2}$2) GaN templates (emission wavelength ≈ 460–560 nm) that have a low and high density of BSFs. The (11$\bar{2}$2) GaN templates with the low BSF density ($<4\times10^{3}$ cm^{-1}) were grown on patterned *r*-plane sapphire substrates.[36] The (11$\bar{2}$2) GaN templates with the high BSF density ($\approx(3.2\pm0.3)\times10^{5}$ cm^{-1}), which

[This article is copyrighted as indicated in the article. Reuse of AIP content is subject to the terms at: http://scitation.aip.org/termsconditions. Downloaded to] IP: 143.239.65.254 On: Thu, 16 Oct 2014 14:24:00

are mainly discussed here, were grown on *m*-plane sapphire.[7,19] Both InGaN quantum wells (≈4–10 nm) and single layers (≈30 nm) with 15%–23% In-content grown on the two different GaN templates show similar RT-PL emission wavelengths indicating that the effect of BSFs on the red-shift of the $(11\bar{2}2)$ InGaN NBE is weak.

The PL peak emission wavelength of the $(11\bar{2}2)$ InGaN layers shows a strong blue-shift (up to ≈60 nm) with increasing excitation power (Fig. 4(a)). The blue-shift might be due to the screening of the built-in electric field and the filling of the band-tail localized states.[33] The PE strongly affects luminescence position of very small structures, e.g., quantum wells and dots, and its effect rapidly decreases with increasing thickness. For the 25–30 nm thick InGaN layers, residual PE exists in the strained and partially relaxed layers, and hence may induce the shift of luminescence. However, as shown in Fig. 4(b), the (0001) InGaN NBE shows almost no shift, irrespective of the excitation source used. Thus, we can neglect the effect of PE in the shift of the $(11\bar{2}2)$ InGaN NBE.

As shown in Fig. 5, the FWHM value of the RT-PL peak wavelength of the InGaN layers increases with decreasing growth temperature, while the RT-PL peak integrated intensity decreases (not shown). The decrease in PL integrated intensity indicates a reduction in the sample quality.

Due to the weak effect of BSFs on the red-shift of the $(11\bar{2}2)$ InGaN NBE with respect to the (0001) InGaN NBE (9.4% ≥ In ≥ 15%), the blue-shift of the $(11\bar{2}2)$ InGaN NBE, and the decrease of the RT-PL FWHM values with increasing excitation power can be explained in the framework of carrier localization-delocalization. To clarify this, we further measured PL spectra together with PLE absorption edge at 12 K using a Xenon lamp excitation source (Fig. 6). The absorption edge positions of the $(11\bar{2}2)$ InGaN layers were determined using a sigmoidal fit.[37] It is worth noting that the indium contents determined by the PLE absorption edge using a bowing parameter of 1.36,[38] and the indium contents determined by XRD measurements (Fig. 2) for the $(11\bar{2}2)$ InGaN layers are in satisfactory agreement between each other.

As shown in Fig. 6(b), a Stokes-shift between PL peak emission wavelength and PLE absorption edge can be observed confirming our previous assumption about the carrier localization in the layers. The Stokes-shift increases from 30 to 200 meV with increasing indium content correlated to the increase of exciton localization. Consequently, the band filling in the localized states induces the blue-shift of the PL peak emission wavelength of the $(11\bar{2}2)$ InGaN layers due to the increase of carrier concentration caused by the increase of excitation power.[33]

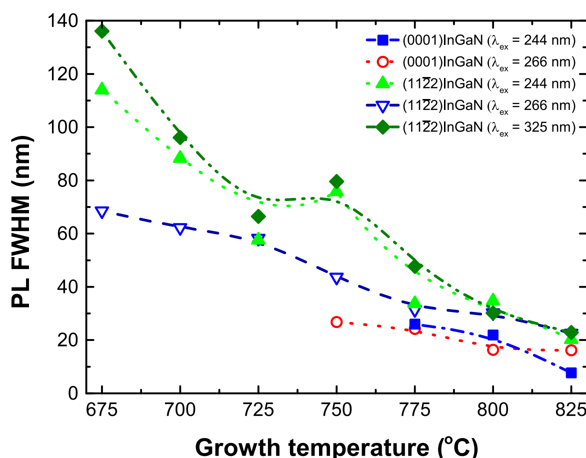

FIG. 5. The FWHM values of the RT-PL spectra measured with different excitation sources of the InGaN layers grown at different temperatures.

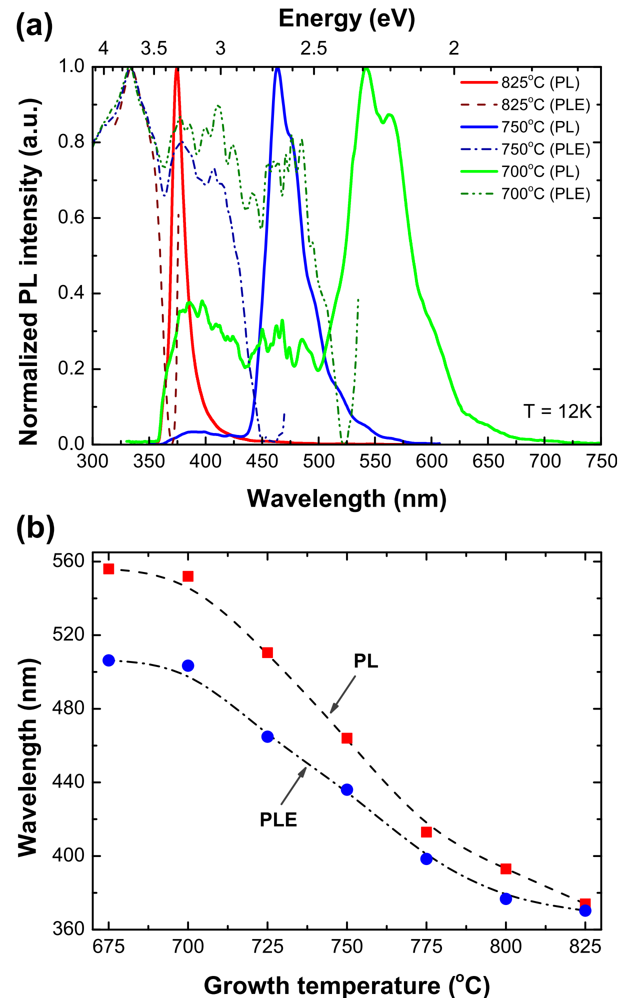

FIG. 6. The LT-PL and PLE spectra (a) and peak emission wavelength (b) measured at 12 K of the $(11\bar{2}2)$ InGaN layers grown at different temperatures.

In this section, the PL properties of the InGaN samples were studied by different excitation wavelengths. At RT, only the fully strained (0001) InGaN layers show clear NBE luminescence when the layers were excited by the 266 nm excitation source. The relaxed (0001) InGaN layers do not emit light due to the increase in defect density/non-radiative centers. In contrast, the $(11\bar{2}2)$ InGaN layers have much higher defect density but the layers have the much stronger PL intensity irrespective of the excitation source used. This was attributed to high background doping and the carrier localization in the layers.

IV. CONCLUSIONS

We have reported on the growth of the InGaN layers simultaneously on (0001) GaN and $(11\bar{2}2)$ GaN templates

[This article is copyrighted as indicated in the article. Reuse of AIP content is subject to the terms at: http://scitation.aip.org/termsconditions. Downloaded to] IP: 143.239.65.254 On: Thu, 16 Oct 2014 14:24:00

using MOVPE. The indium composition of the InGaN layers was found to have a strong dependence on growth temperature. For both $(11\bar{2}2)$ and (0001) InGaN layers, a similar indium content (<15%) was obtained at growth temperature $\geq 750\,^{\circ}C$, while a lower indium content in the $(11\bar{2}2)$ InGaN layers (15%–26%) compared to that of the (0001) InGaN layers grown at the same time (15%–32%) was observed in the lower growth temperature range (675–750 °C). This sharp divergence is attributed to the sudden change in the strain state of the (0001) layers. The strain relaxation of the $(11\bar{2}2)$ InGaN layers correlated with the change of the crystallinity and the tilt angle. The RT-PL peak emission wavelength of the $(11\bar{2}2)$ InGaN layers varied from 380 nm to 580 nm. The blue-shift of the RT-PL peak emission wavelength with increasing excitation power was attributed to band filling effects in the InGaN layers.

ACKNOWLEDGMENTS

This work was financially supported by the EU-FP7 ALIGHT project, under Agreement No. FP7-280587. This work was also partially supported by the Programme for Research in Third Level Institutions (PRTLI) fourth and fifth cycles. S.N.A. acknowledges financial support for his postgraduate fellowship from the Iranian Ministry of Science, Research and Technology. P.J.P. acknowledges financial support for his Professorship from Science Foundation Ireland.

[1]A. E. Romanov, T. J. Baker, S. Nakamura, and J. S. Speck, J. Appl. Phys. **100**, 023522 (2006).
[2]A. Strittmatter, J. E. Northrup, N. M. Johnson, M. V. Kisin, P. Spiberg, H. El-Ghoroury, A. Usikov, and A. Syrkin, Phys. Status Solidi B **248**, 561 (2011).
[3]M. V. Kisin, C. L. Chuang, and H. S. El-Ghoroury, Semicond. Sci. Technol. **27**, 024012 (2012).
[4]H. Sato, A. Tyagi, H. Zhong, N. Fellows, R. B. Chung, M. Saito, K. Fujito, J. S. Speck, S. P. DenBaars, and S. Nakamura, Phys. Status Solidi RRL **1**, 162 (2007).
[5]H. Sato, R. B. Chung, H. Hirasawa, N. Fellows, H. Masui, F. Wu, M. Saito, K. Fujito, J. S. Speck, S. P. DenBaars, and S. Nakamura, Appl. Phys. Lett. **92**, 221110 (2008).
[6]T. Gühne, Z. Bougrioua, P. Vennégués, M. Leroux, and M. Albrecht, J. Appl. Phys. **101**, 113101 (2007).
[7]C. F. Johnston, M. A. Moram, M. J. Kappers, and C. J. Humphreys, Appl. Phys. Lett. **94**, 161109 (2009).
[8]H. Jönen, U. Rossow, H. Bremers, L. Hoffmann, M. Brendel, A. D. Drager, S. Schwaiger, F. Scholz, J. Thalmair, J. Zweck, and A. Hangleiter, Appl. Phys. Lett. **99**, 011901 (2011).
[9]K. H. Baik, Y. G. Seo, S. K. Hong, S. G. Lee, J. B. Kim, J. S. Son, and S. M. Hwang, IEEE Photonics Technol. Lett. **22**, 595 (2010).
[10]J. E. Northrup, Appl. Phys. Lett. **95**, 133107 (2009).
[11]M. V. Durnev, A. V. Omelchenko, E. V. Yakovlev, I. Y. Evstratov, and S. Y. Karpov, Appl. Phys. Lett. **97**, 051904 (2010).
[12]M. V. Durnev, A. V. Omelchenko, E. V. Yakovlev, I. Y. Evstratov, and S. Y. Karpov, Phys. Status Solidi A **208**, 2671 (2011).
[13]Y. Zhao, Q. Yan, C. Y. Huang, S. C. Huang, P. S. Hsu, S. Tanaka, C. C. Pan, Y. Kawaguchi, K. Fujito, C. G. Van de Walle, J. S. Speck, S. P. DenBaars, S. Nakamura, and D. Feezell, Appl. Phys. Lett. **100**, 201108 (2012).
[14]T. Wernicke, L. Schade, C. Netzel, J. Rass, V. Hoffmann, S. Ploch, A. Knauer, M. Weyers, U. Schwarz, and M. Kneissl, Semicond. Sci. Technol. **27**, 024014 (2012).
[15]H. Jönen, H. Bremers, U. Rossow, T. Langer, A. Kruse, L. Hoffmann, J. Thalmair, J. Zweck, S. Schwaiger, F. Scholz, and A. Hangleiter, Semicond. Sci. Technol. **27**, 024013 (2012).
[16]A. Das, S. Magalhaes, Y. Kotsar, P. K. Kandaswamy, B. Gayral, K. Lorenz, E. Alves, P. Ruterana, and E. Monroy, Appl. Phys. Lett. **96**, 181907 (2010).
[17]D. A. Browne, E. C. Young, J. R. Lang, C. A. Hurni, and J. S. Speck, J. Vac. Sci. Technol., A **30**, 041513 (2012).
[18]F. Oehler, M. E. Vickers, M. J. Kappers, and R. A. Oliver, J. App. Phys. **114**, 053520 (2013); **114**, 219901 (2013).
[19]M. J. Kappers, J. L. Hollander, C. McAleese, C. F. Johnston, R. F. Broom, J. S. Barnard, M. E. Vickers, and C. J. Humphreys, J. Cryst. Growth **300**, 155 (2007).
[20]J. Bai, T. Wang, P. J. Parbrook, I. M. Ross, and A. G. Cullis, J. Cryst. Growth **289**, 63 (2006).
[21]M. A. Moram and M. E. Vickers, Rep. Prog. Phys. **72**, 036502 (2009).
[22]S. Ploch, T. Wernicke, D. V. Dinh, M. Pristovsek, and M. Kneissl, J. Appl. Phys. **111**, 033526 (2012).
[23]D. V. Dinh, D. Skuridina, S. Solopow, M. Frentrup, M. Pristovsek, P. Vogt, M. Kneissl, F. Ivaldi, S. Kret, and A. Szczepańska, J. Appl. Phys. **112**, 013530 (2012).
[24]J. E. Northrup and J. Neugebauer, Phys. Rev. B **60**, R8473 (1999).
[25]X. Niu, G. B. Stringfellow, and F. Liu, Appl. Phys. Lett. **99**, 213102 (2011).
[26]M. Moret, S. Ruffenach, O. Briot, and B. Gil, Phys. Status Solidi A **208**, 1183 (2011).
[27]J. Stellmach, F. Mehnke, M. Frentrup, C. Reich, J. Schlegel, M. Pristovsek, T. Wernicke, and M. Kneissl, J. Cryst. Growth **367**, 42 (2013).
[28]T. Ogino and M. Aoki, Jpn. J. Appl. Phys., Part 1 **19**, 2395 (1980).
[29]E. G. Schubert, I. D. Goepfert, and J. M. Redwing, Appl. Phys. Lett. **71**, 3224 (1997).
[30]I. H. Lee, J. J. Lee, P. Kung, F. J. Sanchez, and M. Razeghi, Appl. Phys. Lett. **74**, 102 (1999).
[31]G. Pozina, S. Khromov, C. Hemmingsson, L. Hultman, and B. Monemar, Phys. Rev. B **84**, 165213 (2011).
[32]S. R. Xu, Y. Hao, J. C. Zhang, Y. R. Cao, X. W. Zhou, L. A. Yang, X. X. Ou, K. Chen, and W. Mao, J. Cryst. Growth **312**, 3521 (2010).
[33]K. Kazlauskas, G. Tamulaitis, J. Mickevicius, E. Kuokstis, A. Zukauskas, Y. C. Cheng, H. C. Wang, C. F. Huang, and C. C. Yang, J. Appl. Phys. **97**, 013525 (2005).
[34]T. Hino, S. Tomiya, T. Miyajima, K. Yanashima, S. Hashimoto, and M. Ikeda, Appl. Phys. Lett. **76**, 3421 (2000).
[35]M. E. Levinshtein, S. L. Rumyantsev, and M. S. Shur, *Properties of Advanced Semiconductor Materials GaN, AlN, InN, BN, SiC, SiGe*, (John Wiley & Sons, Inc., New York, 2001).
[36]F. Scholz, T. Meisch, M. Caliebe, S. Schörner, B. Neuschl, K. Thonke, L. Kirste, S. Bauer, S. Lazarev, and T. Baumbach, J. Cryst. Growth **405**, 97 (2014).
[37]R. W. Martin, P. G. Middleton, K. P. O'Donnell, and W. Van der Stricht, Appl. Phys. Lett. **74**, 263 (1999).
[38]P. G. Moses and C. G. Van de Walle, Appl. Phys. Lett. **96**, 021908 (2010).

[This article is copyrighted as indicated in the article. Reuse of AIP content is subject to the terms at: http://scitation.aip.org/termsconditions. Downloaded to] IP: 143.239.65.254 On: Thu, 16 Oct 2014 14:24:00